Review Article

Emerging Applications for Ferumoxytol as a Contrast Agent in MRI

Mustafa R. Bashir, MD,* Lubna Bhatti, MBBS, Daniele Marin, MD, and
Rendon C. Nelson, MD

Ferumoxytol is an ultrasmall superparamagnetic iron oxide (USPIO) agent initially approved by the Food and Drug Administration (FDA) as an iron replacement therapy for patients with anemia due to chronic renal failure. Recently, ferumoxytol has been investigated extensively as an intravenous contrast agent in magnetic resonance imaging (MRI). Since it causes regional T_1 and T_2* shortening in vivo, conventional pulse sequences can be used following ferumoxytol administration to demonstrate signal enhancement or loss. Ferumoxytol can be administered as a rapid bolus and has a long intravascular half-life on the order of 14–15 hours, making it a potentially useful agent for vascular and perfusion-weighted MRI. In comparison to other USPIOs, ferumoxytol is less limited by allergic and idiosyncratic reactions. Furthermore, since ferumoxytol is an iron-based agent with no potential for causing nephrogenic systemic fibrosis, it may be useful as an alternative to gadolinium-based contrast agents in patients with compromised renal function. Ferumoxytol is ultimately taken up by macrophages/the reticuloendothelial system in the liver, spleen, and lymph nodes, and this uptake mechanism is being explored as a novel imaging technique for vascular lesions, tumors, and lymph nodes. This article reviews the properties of ferumoxytol relevant to MRI as well as many of the uses for the agent currently under investigation.

Key Words: ferumoxytol; feraheme; SPIO; USPIO
J. Magn. Reson. Imaging 2015;41:884–898.
© 2014 Wiley Periodicals, Inc.

MAGNETIC RESONANCE IMAGING (MRI) is a collection of powerful techniques that are widely applied throughout medical imaging. Traditional MRI pulse sequences (T_1-weighted, T_2-weighted, proton density, T_2*/susceptibility-weighted) depict regional differences in tissue composition, and can provide both static and dynamic data regarding tissue structure. Many applications, particularly oncologic and cardiovascular MRI, benefit from the intravenous infusion of extrinsic contrast agents. Contrast-enhanced MRI (ceMRI) and magnetic resonance angiography (MRA) provide improved depiction of large- and medium-sized vessels and can demonstrate the dynamic vascular/perfusional properties of tissues (1–5). The information gleaned following contrast media injection depends on both the vascular and interstitial characteristics of the tissue in question, as well as the expected distribution of the contrast material. Most commercially available contrast agents are small molecular weight molecules that distribute in a "nonspecific" manner between the intravascular and interstitial compartments of the extracellular space. Some of these agents are also taken up selectively by particular tissues, such as hepatocytes or the reticuloendothelial system (6,7). Still other agents, which are large macromolecular compounds, are relatively confined to the intravascular compartment, and are referred to as blood pool agents (8–10).

Most of the contrast agents widely available for use in MRI are based on gadolinium, a rare earth metal which is bound within an organic chelate molecule. In the past, these agents were thought to be associated with very few adverse events, beyond the small risks of idiosyncratic and rare anaphylactoid reactions (11). Gadolinium-based contrast agents (GBCAs) were frequently administered at two or three times the approved dose in order to achieve high image quality and levels of enhancement, for example, for MRA. In time, however, nephrogenic system fibrosis (NSF) was described and found to be associated with or caused by GBCA administration in most cases (12–16). Nephrogenic systemic fibrosis is a potentially morbid and deadly disease characterized by soft-tissue contractures and occasionally cardiopulmonary compromise. The occurrence of this disease was found to be associated with high-dose GBCA administration, renal dysfunction, and other risk factors (11). Despite being a rare disease relative to the number of GBCA doses administered worldwide, NSF nonetheless gained a great deal of attention, in part due to its iatrogenic nature, and in part because it represents an important complication related to a medication which was previously thought to be relatively safe.

Table 1
Potential Clinical Applications for Ferumoxytol as a Contrast Agent in MRI

Application	Type	Reference numbers
Aortic imaging	GBCA alternative	8, 35–38
Transplant renal artery	GBCA alternative	41
Arteriovenous fistula	GBCA alternative	42
Deep vein thrombosis	GBCA alternative	10, 20, 44, 45
Hepatic parenchymal lesions	GBCA alternative	50–53 (extrapolated)
Brain tumors	Macrophage uptake	4, 30, 55–56
Intracranial vascular malformations	GBCA alternative and macrophage uptake	57–65
Arterial plaque stability	Macrophage uptake	74–82
Lymph node imaging	Macrophage uptake	86–94
Perfusion imaging	GBCA alternative	95–97
Islet cell labeling	Cellular uptake	100–101 (extrapolated)
Stem cell labeling	Cellular uptake	102–103

With more judicious GBCA dosing, careful attention to patient risk factors, and use of GBCAs with relatively favorable safety profiles, the incidence of NSF appears to have fallen substantially. Nonetheless, awareness of this disease has prompted active interest in nongadolinium-based contrast agents. Several such agents had previously been available and were not associated with NSF, although they had strengths and weaknesses of their own. For example, MN-DPDP (Teslascan, Nycomed, Amersham, Piscataway, NJ) is taken up by the hepatocytes and provided high-quality images differentiating hepatocyte-containing and nonhepatocyte-containing tissues. However, dynamic imaging was challenging with this agent because of the relatively high recommended flow rates (up to 4–6 mL/sec) and the frequency of transient flushing, warmth, and headache associated with bolus administration. Iron-based agents such as ferumoxides (Feridex, Advanced Magnetics, Cambridge, MA) are taken up by the reticuloendothelial system, but some could not be administered as an intravenous bolus due to associated severe back pain. Other iron-based agents have been investigated in humans; however, they currently have limited commercial availability.

Ferumoxytol (Feraheme, AMAG Pharmaceuticals, Cambridge, MA) is a commercially available ultrasmall superparamagnetic iron oxide (USPIO) agent used as an iron replacement therapy for patients with anemia related to chronic renal insufficiency. As an iron-based agent, it carries no risk of NSF, and causes enhancement on T_1-weighted images by shortening the T_1 relaxation time of adjacent nuclei. It can be administered via bolus intravenous injection, and initially behaves as a blood pool agent, making it a potential alternative to GBCAs for some imaging applications. The agent is also taken up by macrophages and ultimately the reticuloendothelial system, opening the door for novel imaging approaches to evaluating lymph nodes and certain tumors.

The purpose of this article is to review the use of ferumoxytol as an intravenous contrast agent in MRI. We will review the properties of the agent and discuss injection and pulse sequence parameters. A variety of specific applications will also be discussed and illustrated. For reference, Table 1 lists the applications covered along with references relevant to each application.
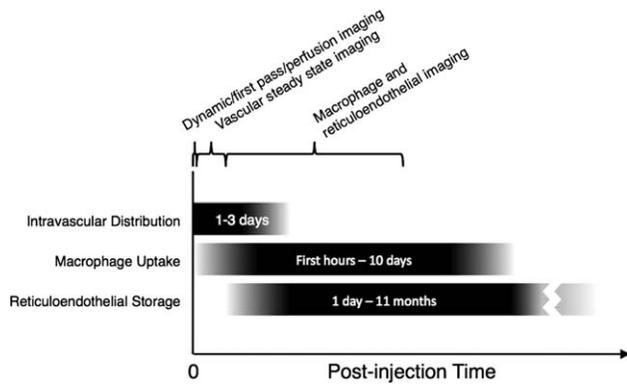
PHYSICAL PROPERTIES
Relaxivity and Biodistribution

In MRI, traditional paramagnetic contrast agents shorten the T_1, T_2, and T_2* relaxation times of local tissues. Their presence and relative concentration in tissue is primarily visualized signal enhancement on T_1-weighted imaging. Their relaxivities are characterized as r_1 and r_2, which reflect their effects on T_1 and T_2 times, respectively. Although r_2* relaxivity (susceptibility) is rarely reported quantitatively, and the relationship between r_2 and r_2* is complex, they are both strongly correlated with the concentration of susceptibility-inducing materials (17). Therefore, we will consider r_2 values as surrogates for r_2* herein.

For most GBCAs, r_1 values typically range from 3.6–5.2 L mmol^{-1} s^{-1} and r_2 values range from 4.3–6.1 L mmol^{-1} s^{-1} in plasma at 37°C and 1.5T (18). Those GBCAs that bind to plasma proteins, at least transiently, exhibit higher values, ranging up to r_1 of 19 L mmol^{-1} s^{-1} and r_2 of 34 L mmol^{-1} s^{-1} (gadofosveset disodium, Lantheus Medical Imaging, Billerica, MA) (18). Ferumoxytol demonstrates a similarly high r_1 relaxivity of 15 L mmol^{-1} s^{-1}, but with a much higher r_2 relaxivity of 89 L mmol^{-1} s^{-1} (19). Thus, ferumoxytol causes strong enhancement on T_1-weighted images, but also can cause strong susceptibility effects.

Ferumoxytol is comprised of iron oxide particles surrounded by a carbohydrate coat. Following intravenous injection, ferumoxytol initially behaves as a blood pool agent, distributing only in the intravascular compartment. Due to its relatively large molecular size (around 750 kDa), there is little leakage of the agent into the extravascular/interstitial compartment and little renal clearance (20). The agent remains at a relatively steady concentration within the intravascular space for several hours (with a circulating half-life of 14–15 hours), providing a long temporal window for high resolution, high signal-to-noise vascular imaging

Figure 1. Schematic summarizing the distribution and key imaging timing for ferumoxytol.

(21). It is then gradually cleared by macrophages from the blood pool over a period of several days, and subsequently broken down.

Following macrophage breakdown, the remaining iron oxide particles are taken up by the reticuloendothelial system, in particular the liver, spleen, and bone marrow. MRI-based methods have demonstrated measurable amounts of residual iron in the liver for months following ferumoxytol administration in healthy volunteers, with clearance times ranging from 3 to more than 11 months (22). Practitioners should be aware of the potential effects on MRI examinations after ferumoxytol administration, as they can confound the interpretation of these examinations (23,24). A schematic summarizing the distribution of ferumoxytol and key timing for imaging after intravenous injection is shown in Fig. 1.

Safety Profile

In Phase II and III clinical trials, ferumoxytol administration was associated with a low adverse event rate (5.2% vs. 4.5% for placebo) (25). The most common adverse events included nausea, dizziness, and diarrhea (25). Since then, a few more serious reactions, particularly hypotension and anaphylaxis, have been reported (26,27). Overall, ferumoxytol has a favorable safety profile; however, practitioners must be aware of these potential side effects. In addition, most trials to date have reported experiences in the population in which ferumoxytol was approved for administration, namely, those with anemia associated with chronic renal disease. No large trials reporting ferumoxytol administration in other populations have been published, thus the side effect profile of the agent in the general population as well as the long-term effects are as yet unknown.

Caution is particularly urged in the pregnant and breast-feeding populations. Ferumoxytol is classified as Pregnancy Category C (as are GBCAs) by the United States Food and Drug Administration (28). Small animal trials have linked ferumoxytol administration (at very high doses) to birth defects, including soft-tissue malformations and decreased fetal weights (28). To date, human data are unavailable; however, the existing animal data suggest that ferumoxytol

should not be administered during pregnancy. By comparison, iodinated contrast agents are classified as Pregnancy Category B and have a more favorable safety profile in pregnancy (29). Thus, for pregnant patients, noncontrast imaging is preferred, and alternative modalities such as computed tomography (CT) should be considered when contrast-enhanced imaging is necessary, for example, in cases of trauma.

Data on ferumoxytol excretion in human breast milk is not currently available, thus the safety implications of administering the agent to breast-feeding women is unknown. However, it has been shown that only a tiny amount of GBCA administered intravenously to the mother is expressed in the breast milk (less than 0.04% over 24 hours), and even less is absorbed by the infant gastrointestinal tract (30–32). Thus, GBCAs may be relatively safe for administration to breast-feeding mothers. Those who desire additional precautions may pump and discard breast milk for 24 hours after GBCA administration to further reduce infant exposure (11).

Because of its extensive evaluation in patients on dialysis or with nondialysis-dependent renal dysfunction, ferumoxytol's primary role in imaging may be in this population, one in which GBCA administration is contraindicated. In these patients, ferumoxytol can be used for a variety of imaging indications and can supplement noncontrast MRI by depicting both large and small vessel enhancement.

TECHNIQUE CONSIDERATIONS

Perhaps the most important physical difference between ferumoxytol and conventional GBCAs is its strong susceptibility effect. At high ferumoxytol concentrations, this effect can cause signal loss, rather than enhancement, on T_1-weighted images, depending on the main magnetic field strength and echo time (TE) of the pulse sequence. Although such signal loss has also been described with GBCAs, it is usually seen only at the injection site prior to dilution of the agent in the blood pool, or in locations where the agent achieves a high concentration such as the urinary bladder (33). With ferumoxytol administration, susceptibility-related signal loss can occur in the abdominal aorta and even the portal vein during the first pass of the contrast bolus (34).

The optimal dilution scheme for ferumoxytol for in vivo imaging has yet to be determined. Phantom studies have shown that, in normal saline and with T_1-weighted sequences with echo times ranging from 1.2–1.7 msec at 1.5T, ferumoxytol produces enhancement up to dilutions of 1:128, using fixed acquisition parameters. At lower dilution factors (higher concentration), ferumoxytol produces gradually less enhancement, with complete signal loss at a factor of 1:16 (35). In a "normal"-sized 75 kg human with an intravascular volume of 3.5 L, this suggests that maximal blood pool enhancement can be produced with the administration of ~27 mL of ferumoxytol; note that the clinical dose of ferumoxytol for treatment of iron-deficiency anemia is a total of 34 mL given in two

Table 2

Example Pulse Sequence Parameters for Performing MRA and Non-MRA Acquisitions Using a 3D T_1-Weighted Pulse Sequence With Ferumoxytol

	1.5T		3T	
	MRA	Non-MRA	MRA	Non-MRA
Repetition time (msec)	3.0	4.2	3.0	3.9
Echo time (msec)	1.1	2.1	1.1	1.3
Flip angle (degrees)	25	12	25	12
Slice thickness (mm)	1.1	4	1.1	4
Acquisition matrix	384 × 269	256 × 192	384 × 269	256 × 192
Acceleration factor (phase encode, partition)	2, 2	2, 2	2, 2	2, 2

MRA images are acquired using a bolus tracking technique in order to obtain appropriate timing.
Parallel acceleration factors are two-dimensional and shown as phase direction acceleration factor x partition direction acceleration factor.

administrations, 1 week apart. Also note that these dilution factors apply to the dilution of the bolus in the entire blood volume. Various other works have described administered doses of ferumoxytol ranging from 0.4–5 mg/kg body weight (0.03–0.17 mL ferumoxytol/kg) (35–38).

However, since the concentration of the initial administered bolus is much higher than this prior to circulation and subsequent dilution, intravascular susceptibility artifacts can be observed during the initial dynamic phases. Fananapazir et al (34) describe transient intravascular susceptibility artifacts in the abdominal vasculature that were strongly associated with a more highly concentrated ferumoxytol bolus, which could reduce the apparent enhancement of critical vascular structures during dynamic imaging. Based on that work, a dilution factor of at least 1:5 (0.2 mL ferumoxytol or less mL saline) may minimize these artifacts during dynamic imaging. The total bolus volume can then be adjusted to maintain the total administered amount of ferumoxytol for optimal blood pool phase imaging (after recirculation/dilution in the blood pool). Notably, the pulse sequences used in that study include echo times ranging from 1.8–2.1 msec, while using even shorter echo times might have reduced the incidence and severity of artifacts. In addition, those authors noted no visual difference in the incidence of those susceptibility artifacts between 1.5T and 3T acquisitions, suggesting that the stronger susceptibility effects at 3T may have been mitigated by other effects, such as stronger enhancement related to longer tissue T_1 times at 3T. Of particular note, the minimal efficacious dose of ferumoxytol for dynamic vascular imaging in vivo has not yet been described for either 1.5 or 3T.

Overall, the total doses and dilution factors for ferumoxytol reported in the literature are widely variable. When first-pass dynamic imaging is important, the dilution factor must be chosen carefully to balance the desire for greater enhancement against the risk of susceptibility artifacts. For blood pool imaging, total administered dose is the most important consideration. There is, however, consensus that using pulse sequences with short echo times and strong T_1-weighting is important to optimize enhancement.

Example pulse sequence parameters are provided in Table 2 for MRA and non-MRA T_1-weighted acquisitions at 1.5T and 3T.

CLINICAL APPLICATIONS

An Alternative to Gadolinium-Based Contrast agents

Aortic Imaging

Extracellular and blood pool GBCAs are frequently used to perform contrast-enhanced (ce)MRA of the great vessels (1–3). In patients with stage 4 or 5 chronic kidney disease (CKD) requiring dialysis, ferumoxytol can be used as an alternative contrast agent when performing aortic MRA (8,38). As a blood pool contrast agent, ferumoxytol provides a much longer temporal window for data acquisition than extracellular agents, allowing imaging to be performed repeatedly beginning as early as the arterial phase and continuing into later phases. This could be of use in imaging of smaller arteries, where extended imaging

Figure 2. Images from T_1-weighted ceMRA examinations of the abdominal aorta performed in patients with atherosclerosis. (**A**) An 89-year-old man with renal insufficiency imaged using ferumoxytol. (**B**) a 71-year-old woman with longstanding hypertension imaged using gadoversetamide, a GBCA. Note excellent delineation of the aortic wall and extensive atherosclerotic plaque, with similar image quality in both cases. Both image sets were acquired in the sagittal plane, processed using a precontrast image mask and cropped to exclude remaining background signal, and displayed as oblique coronal maximum intensity projection images.

Figure 3. Images from T_1-weighted ceMRA examinations of the abdominal aorta performed in patients with aortic dissections. **(A,B)** A 63-year-old man with endstage renal disease imaged using ferumoxytol. **(C,D)** A 59-year-old woman imaged with gadoversetamide. The dissection plane is well delineated on both volume-rendered images (white arrows, A,C) and axial images (white arrows, B,D), allowing precise definition of the course of the dissection. Both image sets were originally acquired in the sagittal plane and displayed using a precontrast image mask.
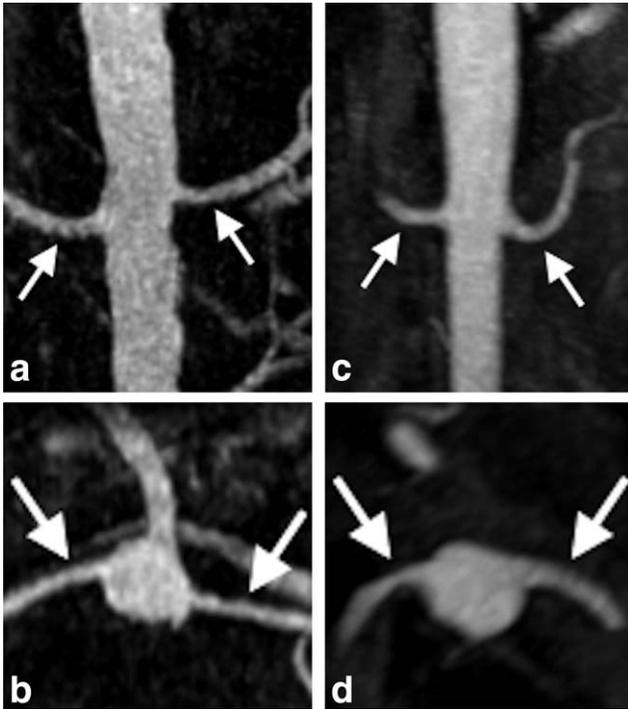
periods could be leveraged to obtain high-resolution imaging with high signal-to-noise ratio (SNR), in applications where venous enhancement can be tolerated. Ferumoxytol has been shown to provide significant increases in SNR and image quality for cardiac, aorta, and pulmonary imaging at 4 mg of iron/kg of body weight, compared with noncontrast MRA (37). Additionally, since extracellular GBCAs are excreted relatively rapidly by the kidneys, their blood pool concentration decreases quickly. In contradistinction, the intravascular concentration of ferumoxytol (and blood pool GBCAs) is relatively constant in the hours following administration, allowing first-pass MRA to be combined with high-quality equilibrium phase MRA (35). Representative images from patients with aortic atherosclerosis and dissections who underwent first-pass MRA of the abdominal aorta with either ferumoxytol or a GBCA are shown in Figs. 2 and 3, respectively.

Detecting aortic endoleaks after endoluminal stent-graft repair can be performed with contrast-enhanced CT angiography or ceMRA. However, like extracellular GBCAs, the iodinated contrast agents used in CT are rapidly excreted, and intravascular signal degrades quickly with time. This creates a clinical dilemma, since low-flow endoleaks may accumulate contrast media slowly, and the optimal imaging time to detect these lesions is controversial. Ferumoxytol has been shown to display small and slow endoleaks, even

hours after injection, due to its long blood pool half-life (36). As part of a phase 2 study, Ersoy et al (36) found that ferumoxytol was useful for detecting subtle, intermittent, or gradual extravasation of blood from the intravascular space (ie, endoleaks) after endoluminal stent-graft repair of infrarenal aortic aneurysms. In that study, ferumoxytol-enhanced MRA delineated the location and volume of endoleak as well as the feeding vessels, information that is extremely important for patient management. Repeated MRA after 24 hours was also useful for calculating the endoleak rate. Therefore, ferumoxytol may have utility in performing both conventional imaging of the aorta as well as delayed imaging.

Native and Transplant Renal Artery Imaging

Chronic renal dysfunction can occur due to a variety of insults, including urinary obstruction, pyelonephritis, diabetes mellitus, medications, and vasculitides. In particular, renal artery stenosis is a relatively common, potentially treatable cause of chronic renal dysfunction in young patients, and the diagnosis is made primarily on the basis of an anatomic imaging modality such as MRA (39). Since these patients, by definition, have some degree of renal dysfunction, the use of ceMRA has fallen for this indication. In this setting, however, ferumoxytol may present a safer alternative for ceMRA of the renal arteries, although its use for
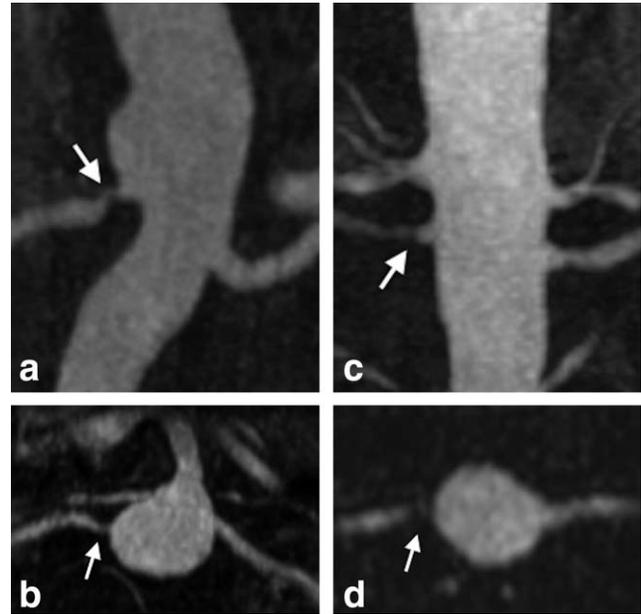
Figure 4. Images from T_1-weighted ceMRA examinations of the renal arteries performed in patients for hypertension, which were negative for renal artery stenosis. Images (**A,B**) A 74-year-old man with chronic renal insufficiency imaged with ferumoxytol. (**C,D**) A 51-year-old woman imaged with gadoversetamide. The right and left renal arteries are well delineated on both oblique coronal (white arrows, A,C) and axial reformatted images (white arrows, B,D), and are widely patent in both patients. Both image sets were originally acquired in the coronal plane and displayed using a precontrast image mask.

this purpose has not yet been formally established. Representative images from patients who underwent renal artery MRA with either ferumoxytol or a GBCA, without and with renal artery stenoses, are shown in Figs. 4 and 5, respectively.

Similarly, vascular compromise by renal artery stenosis or renal vein thrombosis are important, treatable causes of kidney transplant dysfunction (40). The imaging evaluation of kidney transplants focuses on the exclusion of urinary obstruction, followed by assessing patency of the renal artery and vein. Since these patients typically present with elevated serum creatinine levels, contrast-enhanced CT and MRI are both contraindicated; thus, the evaluation is typically performed by ultrasonography. Unfortunately, ultrasonography often provides insufficient information to guide patient care. In such cases, transplant MRA with ferumoxytol has shown utility in establishing the diagnoses of renal artery stenosis and thrombosis noninvasively, and may provide an alternative contrast-enhanced technique when ultrasonography is nondiagnostic (41).

Compared to those with kidney transplants, many patients with severe renal insufficiency are dependent on hemodialysis via a peripheral arteriovenous fistula (AVF). MRA with ferumoxytol has shown some value in the evaluation of AVF patency, since ceMRA using
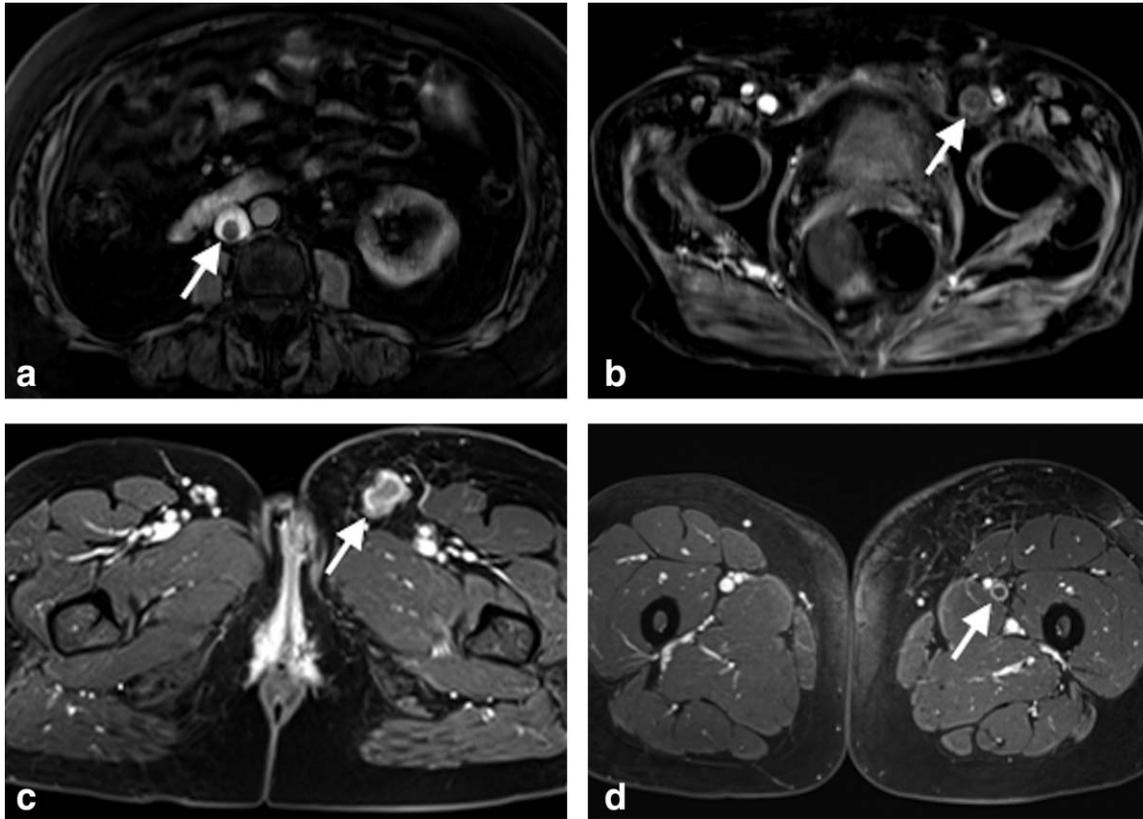

Figure 5. Images from T_1-weighted ceMRA examinations of the renal arteries performed in two patients with hypertensions, demonstrating renal artery stenoses. (**A,B**) A 69-year-old man with end-stage renal disease imaged with ferumoxytol. (**C,D**) A 73-year-old woman imaged with gadoversetamide. High-grade proximal renal artery stenoses are well delineated, involving the single right renal artery in the first patient (white arrows, A,B), and involving the lower pole right renal artery in the second patient (white arrows, C,D), who has duplicated renal arteries bilaterally. Both image sets were originally acquired in the coronal plane and displayed using a precontrast image mask.

GBCAs is contraindicated in this population. While noncontrast time-of-flight MRA is an alternative in these patients, it is time-consuming and prone to artifacts related to susceptibility, slow flow, and vessel tortuosity (42). Ferumoxytol-enhanced ceMRA can provide the advantages of contrast-enhanced imaging without the potential for NSF in this high-risk population (42).

Venous Imaging

Lower extremity deep vein thrombosis (DVT) is a common condition that can cause life-threatening pulmonary embolism as well as a number of extremity complications, including thrombophlebitis and venous insufficiency. The diagnosis is typically made on clinical grounds and confirmed by graded compression ultrasound (43). However, at times thrombosis can be isolated to the deep abdominopelvic veins, or evaluation of abdominopelvic extension of lower extremity thrombosis is needed, and ultrasound cannot reliably assess these venous segments. Contrast-enhanced MR venography (ceMRV) with blood pool contrast agents has been shown to be highly accurate for the diagnosis of abdominopelvic and lower extremity DVT (10,44,45).

Although most of the investigations of ceMRV for DVT detection with blood pool agents have focused on gadofosveset trisodium, ferumoxytol has shown utility in patients both with and without contraindications to

Figure 6. Images from T_1-weighted ceMRV examinations performed using blood pool contrast agents in patients with deep vein thrombosis. (**A,B**) A 68-year-old woman with chronic renal insufficiency imaged with ferumoxytol. (**C,D**) A 56-year-old man imaged with gadofosveset trisodium, a GBCA. Intraluminal filling defects with surrounding enhancement, consistent with acute thromboses, are well visualized in the inferior vena cava (white arrow, A) and left common femoral vein (white arrow, B) of the first patient, and in the left common femoral vein bifurcation (white arrow, C) and left femoral vein (white arrow, D). Note excellent venous enhancement in both cases.

GBCA administration (20,46). In general, ceMRV acquisition is much faster than noncontrast MRV, while providing higher contrast-to-noise ratios (46). In addition, at 1.5T, ferumoxytol-enhanced MRV has been shown to provide quantitatively similar enhancement of patent vessels and similar conspicuity of intravascular thrombi when compared to gadofosveset-enhanced ceMRV in both the abdomino-pelvic and lower extremity deep venous systems (20).

These studies show that ferumoxytol can be an efficacious substitute for GBCAs for ceMRV. In particular, it provides both excellent conspicuity of thrombi and rapid image acquisition, thereby allowing for large anatomic coverages in a clinically feasible amount of time.
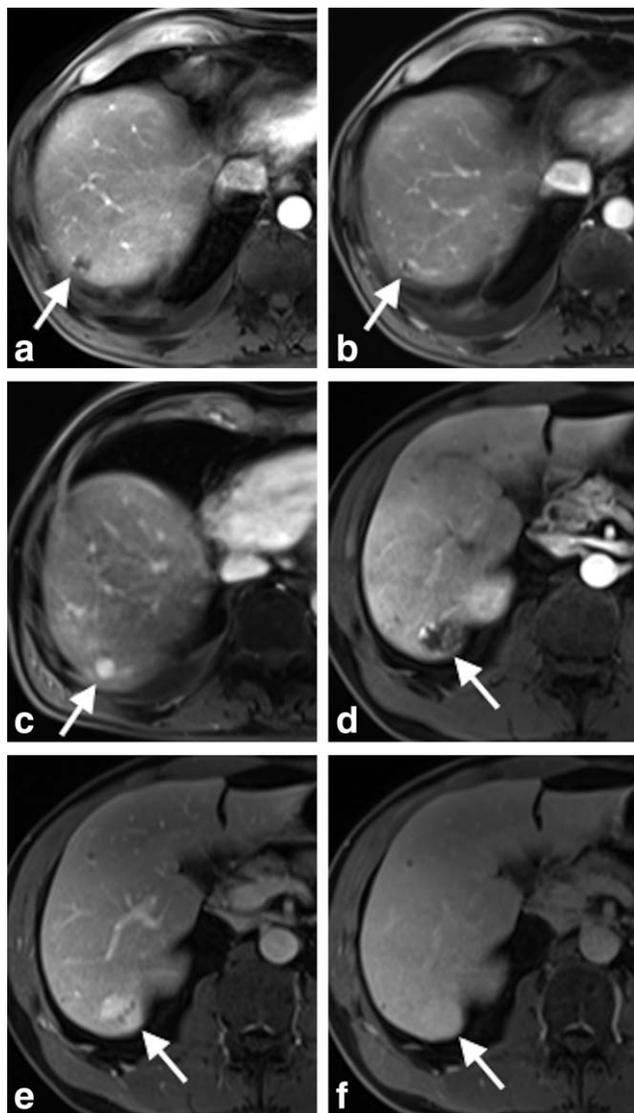
Representative images from ceMRV of the lower extremity deep venous system performed with ferumoxytol or a GBCA are shown in Fig. 6.

Abdominal Parenchymal Imaging

Because it can be administered as a bolus injection, similar to GBCAs, ferumoxytol could be an attractive alternative when there are contraindications to GBCA administration. However, the biodistribution of blood pool agents differs substantially from that of extracellular GBCAs and, as such, they provide somewhat different types of images. In addition, a paucity of data are currently available regarding the use of blood pool agents for solid organ parenchymal evaluation in the abdomen.

Imaging phases based primarily on vascular enhancement, such as the hepatic arterial and portal venous phases, could be realized. However, since ferumoxytol does not equilibrate with the extravascular interstitial space, a blood-pool phase results rather than the equilibrium/interstitial phase typical of extracellular GBCAs. This phase is similar to that realized using the nuclear agent technetium-99m-labeled red blood cells, and may be useful for making the specific diagnosis of cavernous hemangiomas (47–49). One small case series has shown that hemangiomas demonstrate classic enhancement features and delayed contrast media retention when imaged with gadofosveset trisodium, also a blood pool agent, thereby allowing confident differentiation from metastases (50). The same principles may be applicable to ferumoxytol; however, no series systematically describing the appearance of focal liver lesions in these phases with this agent are yet available. Representative dynamic phase images from contrast-enhanced MRIs performed with either ferumoxytol or a GBCA are shown in Fig. 7, in two patients with hepatic hemangiomas.

Figure 7. Images from dynamic contrast-enhanced T_1-weighted MRI examinations of the liver in patients with hepatic hemangiomas. **(A,B)** A 44-year-old man with chronic renal insufficiency imaged using ferumoxytol. **(C,D)** A 38-year-old man imaged with gadobenate dimeglumine, a GBCA. Peripheral nodular enhancement is apparent in both cases in the hepatic arterial (A,D) and portal venous phases **(B,E)**, with complete fill-in of the lesions in the late dynamic phases **(C,F)**, diagnostic of hepatic hemangiomas.

Finally, the utility of several other iron-based agents has been described when imaging is performed after uptake by the reticuloendothelial system (7,51,52). Using T_2- or T_2*-weighted pulse sequences, liver lesions without reticuloendothelial uptake (eg, metastases and most hepatocellular carcinomas) become more conspicuous due to susceptibility-related signal loss from ferumoxytol uptake in the normal background liver (51,52). Additionally, focal nodular hyperplasia is characterized by signal suppression that is similar to the surrounding liver, since the majority of these lesions also take up iron-based agents (53). However, unlike many other iron-based agents, uptake of ferumoxytol by the reticuloendoth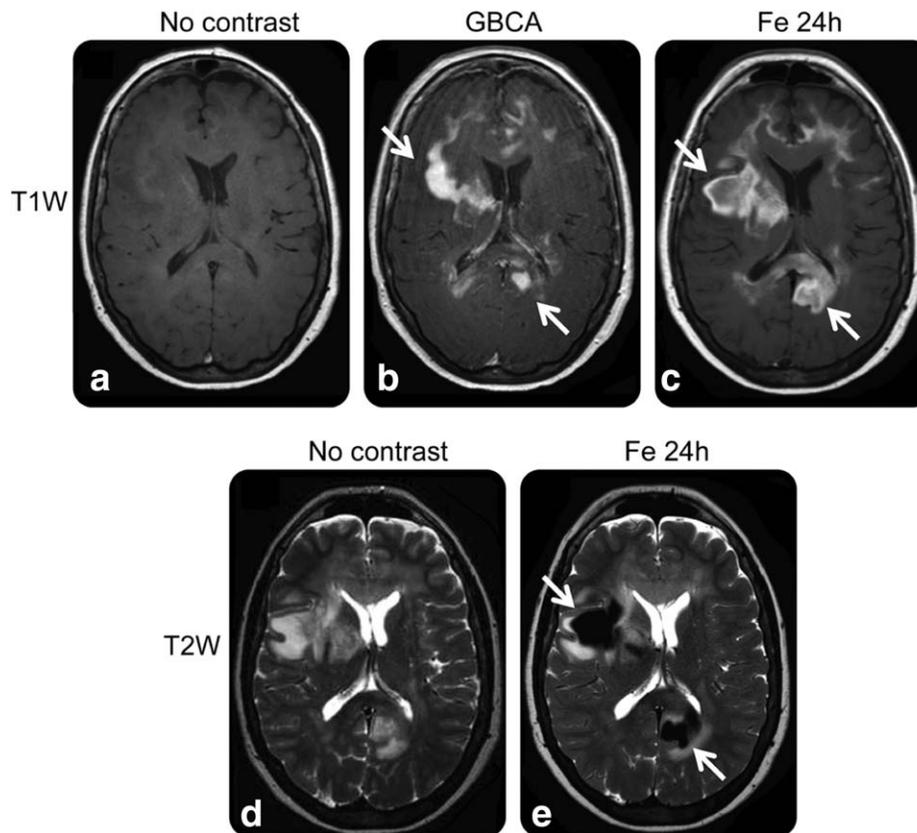elial system may not be immediate, since it must first be taken up and broken down by macrophages. Moreover, although multiple reports have described visible signal loss in the liver and spleen 2 days after administration, the precise timing of and patient-to-patient variability in reticuloendothelial uptake has not yet been elucidated. What is clear is that capturing images during both the vascular and reticuloendothelial phases usually requires multiple imaging sessions, which may not be feasible in a busy clinical practice (21,23,54).

Novel Applications

Imaging of Brain Tumors and Intracranial Vascular Lesions

Ferumoxytol has been investigated for use in both brain tumor and cerebrovascular imaging. Initially, postinjection, high-quality ceMRA images can be acquired. Immediate postcontrast T_1-weighted images can be acquired to demonstrate areas of blood–brain barrier breakdown, although the utility of enhancement in this phase after ferumoxytol administration has not been established and, in at least one study, was inferior to immediate postcontrast enhancement with a GBCA (4). Since it is slowly taken up by macrophages, their distribution can be determined. It has been shown that macrophages are present in some brain tumors, allowing for the differentiation (based on the enhancement pattern) of such lesions such as glial tumors, lymphomas, and inflammation, a common clinical need (55). Hamilton and colleagues (30) found no difference in the size of the enhancing regions on T_1-weighted imaging when comparing gadoteridol (immediately postinjection) to ferumoxytol (at 24 hours postinjection) in untreated glial tumors (56). They also described reduced tumoral enhancement and increased peritumoral enhancement in meningiomas following radiation therapy, a phenomenon which was felt to reflect the posttherapy inflammatory response and changing distribution of macrophage deposition. They also suggested that areas with abundant macrophage deposition could be used to target specific sites for biopsy. Figure 8 shows a comparison of contrast-enhanced imaging using a GBCA and ferumoxytol in a patient with primary central nervous system lymphoma, where an area of ferumoxytol uptake on T_2-weighted imaging was used to target a stereotactic needle biopsy (reproduced with permission (57)).

Intracranial aneurysms (IAs) and arteriovenous malformations (AVMs) are important indications for clinical MRI (58). It has been well shown that the primary pathogenesis in the formation and rupture of IAs is inflammation, and that endothelial cell injury is associated with macrophage migration into aneurysm walls, smooth muscle cell death, and aneurysm wall weakness (59–61). Thus, the ability of ferumoxytol to depict macrophage distribution makes it a logical choice for IA imaging. In a small pilot study, Hasan et al (62) showed that IAs with early uptake (within 24 hours) of ferumoxytol were prone to rupture or increase in size, while IAs with late uptake (72 hours)

Figure 8. Images from a patient with primary central nervous system (CNS) lymphoma. **(A,B)** Precontrast and postcontrast gadolinium-enhanced T_1-weighted images demonstrate multifocal, enhancing, deep white matter lesions (white arrows). Enhancement is heterogeneous and poorly defined. **(C)** A T_1-weighted image obtained 24 hours after intravenous ferumoxytol administration demonstrates more confluent and extensive enhancement, likely related to phagocytic cell uptake, in a similar pattern to the gadolinium-enhanced images. **(D,E)** T_2-weighted images obtained before and 24 hours after intravenous ferumoxytol administration demonstrate several areas of confluent, focal, strong signal loss due to ferumoxytol uptake. Stereotactic needle biopsy of the right frontal T_2-hypointense lesion confirmed the suspected diagnosis of diffuse large B-cell lymphoma. Reproduced with permission from Farrell et al (Neurology 2013;81:256–263).

were stable without rupture, over a 6-month follow-up period. The same group also performed a study to assess the antiinflammatory effects of aspirin on IAs. They found that patients treated with aspirin prior to imaging had decreased ferumoxytol uptake in the aneurysm wall compared to patients treated after imaging. This suggested that aspirin caused a decrease in inflammation, an observation which was corroborated on histopathological specimens (63,64). These findings suggest that ferumoxytol-enhanced MRI could provide a noninvasive prognostic assessment of aneurysm stability, risk-stratify lesions in need of early intervention, and may be useful for following the response to medical therapy.

Inflammation also plays a role in the pathophysiology of AVMs, and ferumoxytol uptake has been demonstrated in AVMs when performed 5 days following administration (65,66). Future studies and additional work is needed to further elucidate the role of inflammatory mediators and, potentially, clinical benefits of such imaging in AVM management.

Arterial Plaque Imaging

Atherosclerotic plaque instability plays a major role in the pathogenesis of cardiovascular diseases such as

myocardial ischemia, acute myocardial infarction, heart failure, and cerebrovascular accidents (67–69). Inflammation is a critical part of plaque initiation and the transition of stable plaque to a vulnerable plaque (69,70). It is well established that vulnerable plaques are rich in macrophages, and are composed of a large lipid core and a thin fibrous cap (71–74). Studies have shown increased uptake of other ultrasmall superparamagnetic particles of iron oxide (USPIO) by in macrophage-rich areas of atherosclerotic plaque, as well as spontaneous USPIO uptake by macrophages in hyperlipidemic rabbits (DDM 43/34, IDF Berlin, Germany) (75–77). In 2003, Kooi et al (78) verified accumulation of USPIOs in macrophages of ruptured and vulnerable atherosclerotic plaques in humans. In 2005, a pilot study in rabbits compared ferumoxtran-10 and ferumoxytol as markers of macrophage burden in atherosclerotic plaque; both agents were effectively taken up by macrophages, and ferumoxytol showed optimum signal intensity 3 days after injection (79).

More recent studies have highlighted the presence of matrix or calcifying vesicle-like structures in highly thrombogenic and unstable atherosclerotic plaques (80–82). Wagner et al (83) demonstrated the

accumulation of very small superparamagnetic iron oxide particles (VSOP) in macrophages and microvesicles of unstable rupture-prone plaques within hour after administration (VSOP C184, Ferropharm, Teltow, Germany). Thus, microvesicles have recently been proposed as a vital marker for destabilized atherosclerotic plaques. Given that macrophage and microvesicle uptake have been demonstrated with a variety of iron-based agents, and ferumoxytol is currently one of the most readily available of such agents, its potential utility in imaging atherosclerotic plaque in humans is very promising.

Lymph Node Imaging

Many primary malignancies spread to the rest of the body via the lymphatic system. The presence of lymphatic metastasis in the sentinel lymph nodes and other regional nodes provides clinically important information regarding tumor staging, treatment options, and patient prognosis (84,85). Conventional CT and MRI have been used to diagnose lymph node metastases, under the assumption that only enlarged or morphologically abnormal nodes contain metastatic disease. However, microscopic metastases disease can exist in normal-appearing lymph nodes, and can go undetected using conventional, morphologic imaging (86).

SPIOs have been used extensively in MRI for staging and nodal evaluation in a variety of malignancies, including head and neck, lung, breast, rectal, and prostate cancer (87–90). These lymphotrophic nanoparticles are taken up by macrophages, which migrate into normal lymph nodes. At imaging, uninvolved nodes demonstrate marked reduction in signal intensity on T_2- and T_2*-weighted images. In lymph nodes partially or completely replaced by metastasis, tumor cell infiltration replace the normal macrophages, preventing localization of SPIOs to the nodes, and the nodes retain their typical signal intensity (87,91). A variety of patterns of lymph node enhancement with SPIOs have been described, ranging from no nanoparticle uptake to homogenous signal loss (88–90). USPIO-enhanced MRI performs well on a per-patient basis as well as on a nodal basis in staging many primary cancers, including prostate, gastric, endometrial, cervical, and breast cancers (87,88,90,92,93).

In particular, Motomura et al (94) showed that USPIO-enhanced MRI accurately stages the sentinel lymph nodes in breast cancer patients, potentially obviating the need for axillary lymph node dissections and sentinel lymph node biopsies. In their study, metastatic lymph nodes predominantly replaced by metastases showed high signal intensity uniform patterns, involving >50% of the node, while uninvolved lymph nodes did not (94). In addition, McDermott et al (95) accurately identified metastatic lymph nodes preoperatively in patients with pancreatic adenocarcinoma, altering the management options for those patients. Ferumoxytol-enhanced MRI in that study increased the sensitivity for detecting malignant nodal involvement from 0–42% (conventional MRI) to 76.5% on a node-by-node basis (95). Based on these studies, USPIO-enhanced MRI has been shown to be a safe and accurate method for determining nodal status/stage in the setting of several primary tumors, thus offering a promising noninvasive imaging technique to improve the preoperative management of these patients. Figure 9 shows examples of normal and metastatic lymph nodes imaged using ferumoxytol in patients with prostate cancer.
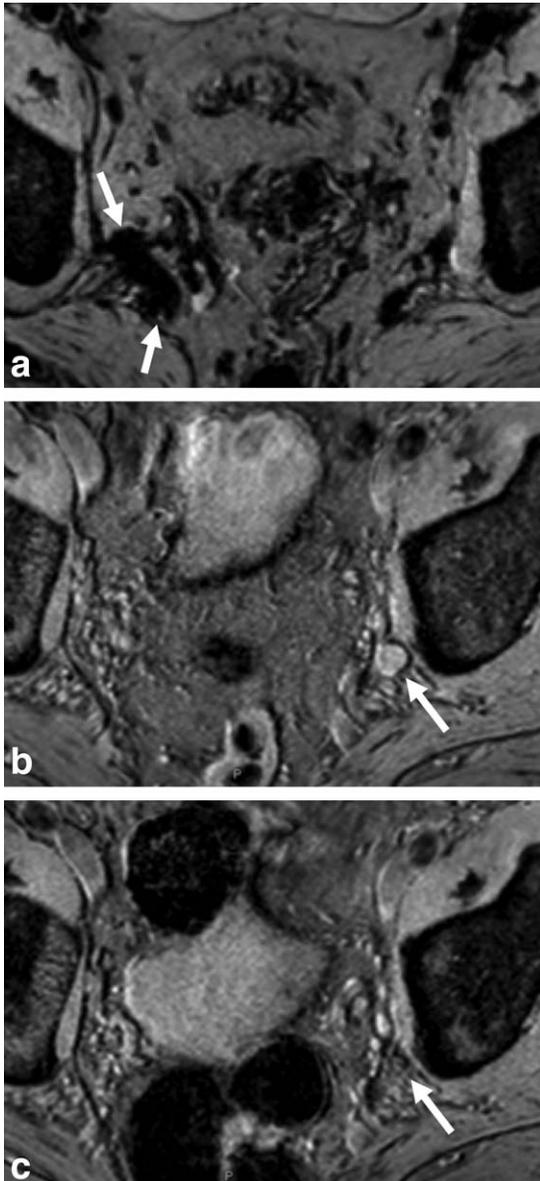
Perfusion Imaging

Dynamic contrast-enhanced first-pass perfusion MRI can lend valuable insight into the blood supply of the brain as well as vascular features of intracranial and extracranial tumors. In the setting of blood–brain barrier disruption, as occurs with neoplasms and inflammation, extracellular GBCAs can leak out of the intravascular compartment, making it possible to characterize tumor perfusion. The calculation of perfusion parameters, however, requires complex modeling to account for the effects of both blood flow and permeability between the intravascular and extravascular extracellular compartments. Using a blood pool agent such as ferumoxytol greatly simplifies the model by eliminating the extravascular space from consideration, thereby providing more robust calculations.

Ferumoxytol has been shown to be an accurate marker of relative cerebral blood volume (rCBV), a marker of tumor vascularity. By comparison, extracellular GBCAs tend to underestimate rCBV (4,96). Measurements of rCBV can be used to monitor decreases in the blood volume and permeability of tumors due to antiangiogenic therapies, and to differentiate true tumor progression from pseudoprogression, an inflammatory phenomenon which mimics true tumor progression at conventional imaging (5,97). A pilot study performed in a pediatric brain tumor population highlighted the successful use of ferumoxytol-enhanced perfusion MRI as a key noninvasive technique in preoperative tumor resection planning, intraoperative tumor localization (in combination with ultrasound), and postoperative evaluation of true tumor progression (98). These studies suggest that ferumoxytol-enhanced perfusion MRI may provide valuable insights and contribute to the clinical care of patients with brain tumors. Figure 10 shows rCBV maps from a patient pseudoprogression of glioblastoma multiforme following chemoradiotherapy; the diagnosis can be made based on low rCBV shown on both ferumoxytol-enhanced and gadolinium-enhanced examinations (reproduced with permission (5)).

Islet and Stem Cell Labeling

Islet cell transplantation is an emerging method for reversing pancreatic insufficiency. Although technically intensive, the insulin-independence rate following islet cell transplantation (an important measure of success of pancreas replacement therapy) approaches that of traditional whole-organ pancreas transplantation (99). Monitoring for rejection, the primary cause of islet cell transplant failure, is more difficult with islet cell transplantation, given the wide distribution

Figure 9. Axial T_2*-weighted images from two patients with prostate cancer imaged 24 hours after intravenous ferumoxytol injection (at a dose of 7.5 mg Fe/kg). (**A**) An image from a 63-year-old man with prostate cancer shows diffuse, homogeneous hypointensity throughout a right pelvic sidewall lymph node (white arrows), consistent with normal ferumoxytol uptake in a benign lymph node. Histopathology demonstrated a benign lymph node. (**B**) An image from a 72-year-old man with recurrent prostate cancer shows maintenance of high signal intensity within a left pelvic sidewall lymph node (white arrow) suggesting metastatic involvement. (**C**) A follow-up image after systemic hormone therapy demonstrates marked reduction in size of the lymph node (white arrow), consistent with treatment response in a metastatic lymph node. Courtesy of Drs. Baris Turkbey and Peter L. Choyke from the Molecular Imaging Program, NCI, NIH, Bethesda, MD.

of transplanted cells throughout the liver and absence of a suitable biopsy target (100). Ex vivo islet cell labeling with ferucarbotran (Resovist, Bayer Healthcare, Wayne, NJ), an SPIO analogous to ferumoxytol, has been described (101). Following transplantation

with labeled islet cells in animals, signal changes in the liver have been shown to correlate with biopsy-proven immune rejection. Graft rescue was successful by increasing immunosuppression in most of those cases, and was initiated based on the signal changes detected by MRI (102). Given that ferucarbotran is no longer commercially available, ferumoxytol may prove a useful alternative agent for this application.

Stem cell transplantation is a promising novel treatment method, in particular for osteoarthritis, an important cause of joint pain related to traumatic injuries and advanced age. Both in vivo and ex vivo labeling of stem cells has been described (103). Ferumoxytol-labeled stem cells have been shown to localize to articular cartilage defects in rats, suggesting that they can be used to monitor cartilage healing (104). The results of these studies suggest that ferumoxytol may be a useful agent for labeling and monitoring various types of cellular transplants.
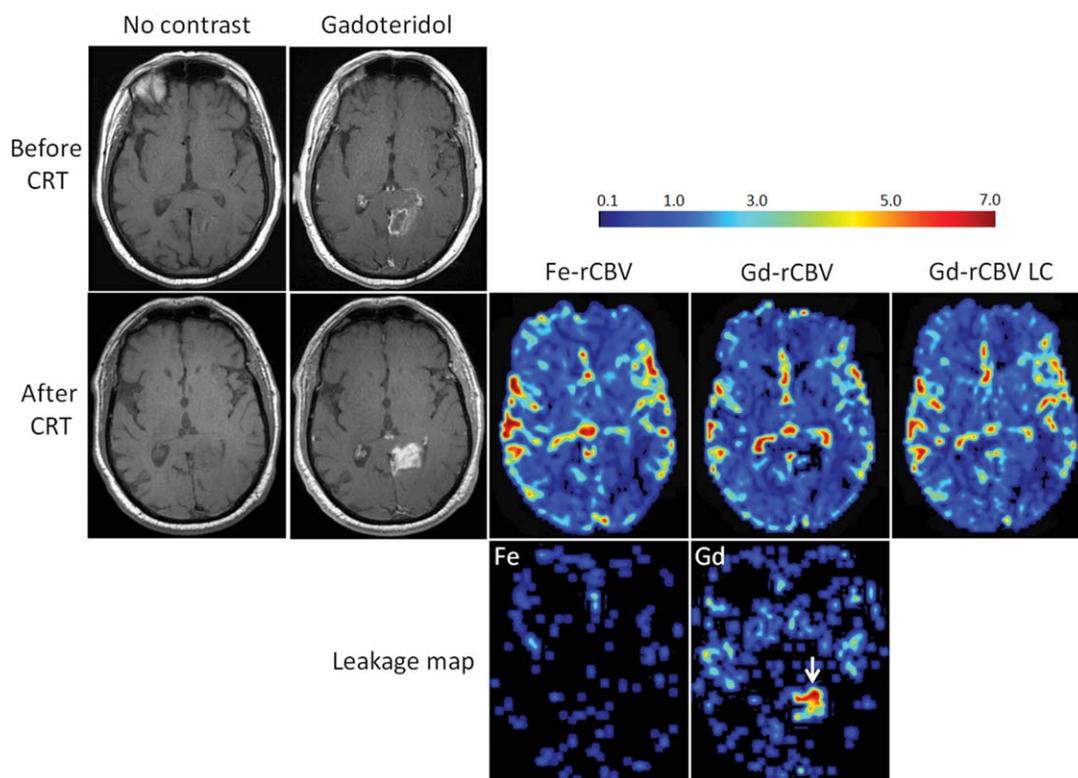
CHALLENGES IN CLINICAL IMAGING WITH FERMOXYTOL

Despite its advantages, some limitations to the use of ferumoxytol remain. First, although it can be used to obtain high-quality dynamic imaging, it must be recognized that ferumoxytol is a blood pool agent, thus the expected enhancement pattern of biological tissues will differ compared with extracellular GBCAs. Furthermore, susceptibility artifacts may be encountered if the administered dose of ferumoxytol and the corresponding pulse sequence parameters are not carefully balanced (34). In addition to the relatively low rate of side effects, some serious reactions have been reported (25,26). Also, some of the applications discussed have been extrapolated from work with other USPIOs or blood pool GBCAs, and although behaviors similar to those of other USPIOs may be expected, direct validation of some of these applications using ferumoxytol is needed.

It is important to note that many of the publications describing the use of ferumoxytol in clinical imaging are either small pilot or proof-of-concept studies. The efficacy of using the agent for various applications still requires validation in larger trials. In addition, head-to-head comparisons are needed with existing techniques, for example, ferumoxytol-enhanced perfusion MRI vs. arterial spin labeling-based perfusion methods. Nonetheless, there are a large number of exciting potential uses for the agent in clinical imaging.

SUMMARY

Although not approved or originally developed as a contrast agent for MRI, ferumoxytol shows great potential for a number of applications. It can be substituted as a blood pool contrast agent for ceMRA of both the arterial and venous systems in patients in whom GBCA administration is unsuitable. Renal allograft and hemodialysis fistula evaluation has been described, applications which, by definition, occur in patients at particularly high risk for NSF. In addition,

Figure 10. Axial images of a 73-year-old man with GBM show pseudoprogression of disease. T_1-weighted MR images without contrast enhancement and with gadoteridol (Gd) obtained before and 3 months after chemoradiotherapy (CRT) show increased contrast enhancement after treatment. Low rCBV (≤ 1.75) is apparent on parametric maps obtained by using ferumoxytol (Fe-rCBV), gadoteridol (Gd-rCBV), and gadoteridol with leakage correction (Gd-rCBV LC), which indicates pseudoprogression. Leakage map shows absence of contrast extravasation when ferumoxytol (Fe) was used and contrast leakage with gadoteridol (arrow). Reproduced with permission from Gahramanov et al (Radiology 2013;266:842–851, copyright Radiological Society of North America).

ferumoxytol's particular distribution with macrophages allows for novel imaging methods not typically performed with GBCAs, including imaging of rupture-prone vascular lesions, lymph node imaging, and cell labeling. Many of these applications have been evaluated only in animals or in small human case series, and additional studies will be needed to translate some of these promising uses into clinical practice.

APPENDIX: CME QUESTIONS

1. Relative to gadolinium-based contrast agents, ferumoxytol has which of the following combination of properties:

   a. High r_1 relaxivity and high r_2 relaxivity
   b. High r_1 relaxivity and low r_2 relaxivity
   c. Low r_1 relaxivity and high r_2 relaxivity
   d. Low r_1 relaxivity and low r_2 relaxivity
  Answer:
  a. Relative to gadolinium-based contrast agents, ferumoxytol has a high r_1 relaxivity (15 L mmol^{-1} s^{-1}

compared with 3.6–19 L mmol^{-1} s^{-1} in plasma at 37°C and 1.5T) and high r_2 relaxivity (89 L mmol^{-1} s^{-1} compared with 4.3–34 L mmol^{-1} s^{-1} in plasma at 37°C and 1.5T). This results in strong signal enhancement on T_1-weighted imaging, but strong signal loss on T_2-weighted imaging. Ferumoxytol also causes strong susceptibility and rapid signal decay on T_2*-weighted images.

2. Initially after intravenous administration, the biodistribution of ferumoxytol most closely resembles which of the following:

   a. Extracellular agent
   b. Blood pool agent
   c. Hepatobiliary agent
   d. Myelin-specific agent

  Answer:
  b. Immediately after intravenous administration, ferumoxytol distributes only in the intravascular compartment, similar to other blood pool agents.

3. In the days to weeks following intravenous administration, ferumoxytol is broken down by / taken up by:

   a. Astrocytes/neuronal cells
   b. Hepatocytes/hepatobiliary system

c. T-cells/bone marrow

d. Macrophages/reticuloendothelial system

Answer:

d. Following intravenous infusion, ferumoxytol is cleared from the blood pool and broken down by macrophages over a period of 1–2 weeks, with the remaining iron oxide particles taken up by the reticuloendothelial system, in particular the liver, spleen, and bone marrow.

4. Which of the following is the proposed mechanism for iron oxide deposition in vulnerable plaque, intracranial aneurysms, and arteriovenous malformations:

a. Regenerating neuronal tissue tends to accumulate iron oxides

b. Vascular lesions prone to rupture tend to be inflamed and rich in macrophages

c. Iron oxides are incorporated into the calcified matrix of chronic vascular lesions

d. Lymph nodes associated with vascular lesions accumulate ferumoxytol

Answer:

b. Inflammation is thought to play a key role in the destabilization of vascular lesions in general, and the transition of stable plaque to vulnerable plaque. Iron oxide agents have been shown to localize to the macrophage-rich areas of these unstable lesions.

5. Interest in iron oxide agents in oncologic imaging has primarily centered around which of the following:

a. More accurate local staging

b. Detection of metastatic disease

c. Identifying lymph nodes with micrometastatic disease

d. Delineating vascular involvement by tumor

Answer:

c. Accurate lymph node staging based on morphology alone can be challenging. Several studies have suggested that ferumoxytol administration may facility the identification of lymph nodes that are involved by metastases but have not yet displayed gross morphologic changes.

REFERENCES

1. Rajagopalan S, Prince M. Magnetic resonance angiographic techniques for the diagnosis of arterial disease. Cardiol Clin 2002; 20:501–512, v.

2. Rengier F, Geisbusch P, Vosshenrich R, et al. State-of-the-art aortic imaging. Part I. Fundamentals and perspectives of CT and MRI. Vasa 2013;42:395–412.

3. Schubert R. Coarctation of the abdominal aorta: demonstration of a rare anomaly using contrast-enhanced MR-angiography. Vasa 2009;38:66–71.

4. Dosa E, Guillaume DJ, Haluska M, et al. Magnetic resonance imaging of intracranial tumors: intra-patient comparison of gadoteridol and ferumoxytol. Neuro Oncol 2011;13:251–260.

5. Gahramanov S, Muldoon LL, Varallyay CG, et al. Pseudoprogression of glioblastoma after chemo- and radiation therapy: diagnosis by using dynamic susceptibility-weighted contrast-enhanced perfusion MR imaging with ferumoxytol versus gadoteridol and correlation with survival. Radiology 2013;266:842–852.

6. Bashir MR, Gupta RT, Davenport MS, et al. Hepatocellular carcinoma in a North American population: does hepatobiliary MR imaging with Gd-EOB-DTPA improve sensitivity and confidence for diagnosis? J Magn Reson Imaging 2013;37:398–406.

7. Gandhi SN, Brown MA, Wong JG, Aguirre DA, Sirlin CB. MR contrast agents for liver imaging: what, when, how. Radiographics 2006;26:1621–1636.

8. Bremerich J, Bilecen D, Reimer P. MR angiography with blood pool contrast agents. Eur Radiol 2007;17:3017–3024.

9. Goyen M. Gadofosveset-enhanced magnetic resonance angiography. Vasc Health Risk Manag 2008;4:1–9.

10. Hadizadeh DR, Kukuk GM, Fahlenkamp UL, et al. Simultaneous MR arteriography and venography with blood pool contrast agent detects deep venous thrombosis in suspected arterial disease. AJR Am J Roentgenol 2012;198:1188–1195.

11. Cohan RH, Davenport MS, Dillman JR, et al. ACR Manual on Contrast Media v8. 2012; Available from: http://www.acr.org/~/media/ACR/Documents/PDF/QualitySafety/Resources/Contrast%20Manual/FullManual.pdf.

12. Broome DR, Girguis MS, Baron PW, Cottrell AC, Kjellin I, Kirk GA. Gadodiamide-associated nephrogenic systemic fibrosis: why radiologists should be concerned. AJR Am J Roentgenol 2007; 188:586–592.

13. Grobner T. Gadolinium—a specific trigger for the development of nephrogenic fibrosing dermopathy and nephrogenic systemic fibrosis? Nephrol Dial Transplant 2006;21:1104–1108.

14. Marckmann P, Skov L, Rossen K, et al. Nephrogenic systemic fibrosis: suspected causative role of gadodiamide used for contrast-enhanced magnetic resonance imaging. J Am Soc Nephrol 2006;17:2359–2362.

15. Sadowski EA, Bennett LK, Chan MR, et al. Nephrogenic systemic fibrosis: risk factors and incidence estimation. Radiology 2007; 243:148–157.

16. Shabana WM, Cohan RH, Ellis JH, et al. Nephrogenic systemic fibrosis: a report of 29 cases. AJR Am J Roentgenol 2008;190: 736–741.

17. Wood JC, Enriquez C, Ghugre N, et al. MRI R2 and R2* mapping accurately estimates hepatic iron concentration in transfusion-dependent thalassemia and sickle cell disease patients. Blood 2005;106:1460–1465.

18. Rohrer M, Bauer H, Mintorovitch J, Requardt M, Weinmann HJ. Comparison of magnetic properties of MRI contrast media solutions at different magnetic field strengths. Invest Radiol 2005; 40:715–724.

19. Corot C, Robert P, Idee JM, Port M. Recent advances in iron oxide nanocrystal technology for medical imaging. Adv Drug Deliv Rev 2006;58:1471–1504.

20. Bashir MR, Mody R, Neville A, et al. Retrospective assessment of the utility of an iron-based agent for contrast-enhanced magnetic resonance venography in patients with endstage renal diseases. J Magn Reson Imaging 2014;40:113–118.

21. McCullough BJ, Kolokythas O, Maki JH, Green DE. Ferumoxytol in clinical practice: Implications for MRI. J Magn Reson Imaging 2013;37:1476–1479.

22. Storey P, Lim RP, Chandarana H, et al. MRI assessment of hepatic iron clearance rates after USPIO administration in healthy adults. Invest Radiol 2012;47:717–724.

23. Schieda N. Parenteral ferumoxytol interaction with magnetic resonance imaging: a case report, review of the literature and advisory warning. Insights Imaging 2013;4:509–512.

24. McCullough BJ, Kolokythas O, Maki JH, Green DE. Ferumoxytol in clinical practice: implications for MRI. J Magn Reson Imaging 2013;37:1476–1479.

25. Pai AB, Garba AO. Ferumoxytol: a silver lining in the treatment of anemia of chronic kidney disease or another dark cloud? J Blood Med 2012;3:77–85.

26. Bailie GR. Comparison of rates of reported adverse events associated with i.v. iron products in the United States. Am J Health Syst Pharm 2012;69:310–320.

27. Santhos S, Podaralla P, Miller B. Anaphylaxis with elevated tryptase after administration of intravenous ferumoxytol. NDT Plus 2010;1322:13–14.

28. Food_and_Drug_Administration. Feraheme Package Insert. 2013 [cited 2013 December 6]; Available from: http://www.accessdata.fda.gov/drugsatfda_docs/label/2009/022180lbl.pdf

29. Food_and_Drug_Administration. Isovue Package Insert. 2013 [cited 2013 December 6]; Available from: http://www.accessdata.fda.gov/drugsatfda_docs/label/2012/018735s054lbl.pdf

30. Kubik-Huch RA, Gottstein-Aalame NM, Frenzel T, et al. Gadopentetate dimeglumine excretion into human breast milk during lactation. Radiology 2000;216:555–558.

31. Rofsky NM, Weinreb JC, Litt AW. Quantitative analysis of gadopentetate dimeglumine excreted in breast milk. J Magn Reson Imaging 1993;3:131–132.

32. Wang PI, Chong ST, Kielar AZ, et al. Imaging of pregnant and lactating patients: part 1, evidence-based review and recommendations. AJR Am J Roentgenol 2012;198:778–784.

33. Neimatallah MA, Chenevert TL, Carlos RC, et al. Subclavian MR arteriography: reduction of susceptibility artifact with short echo time and dilute gadopentetate dimeglumine. Radiology 2000; 217:581–586.

34. Fananapazir G, Marin D, Suhocki PV, Kim CY, Bashir MR. Vascular artifact mimicking thrombosis on MR imaging using ferumoxytol as a contrast agent in abdominal vascular assessment. J Vasc Interv Radiol 2014;25:969–976.

35. Li W, Tutton S, Vu AT, et al. First-pass contrast-enhanced magnetic resonance angiography in humans using ferumoxytol, a novel ultrasmall superparamagnetic iron oxide (USPIO)-based blood pool agent. J Magn Reson Imaging 2005;21:46–52.

36. Ersoy H, Jacobs P, Kent CK, Prince MR. Blood pool MR angiography of aortic stent-graft endoleak. AJR Am J Roentgenol 2004; 182:1181–1186.

37. Prince MR, Zhang HL, Chabra SG, Jacobs P, Wang Y. A pilot investigation of new superparamagnetic iron oxide (ferumoxytol) as a contrast agent for cardiovascular MRI. J Xray Sci Technol 2003;11:231–240.

38. Stabi KL, Bendz LM. Ferumoxytol use as an intravenous contrast agent for magnetic resonance angiography. Ann Pharmacother 2011;45:1571–1575.

39. Leung DA, Hagspiel KD, Angle JF, Spinosa DJ, Matsumoto AH, Butty S. MR angiography of the renal arteries. Radiol Clin North Am 2002;40:847–865.

40. Bruno S, Remuzzi G, Ruggenenti P. Transplant renal artery stenosis. J Am Soc Nephrol 2004;15:134–141.

41. Bashir MR, Jaffe TA, Brennan TV, Patel UD, Ellis MJ. Renal transplant imaging using magnetic resonance angiography with a nonnephrotoxic contrast agent. Transplantation 2013;96:91–96.

42. Sigovan M, Gasper W, Alley HF, Owens CD, Saloner D. USPIO-enhanced MR angiography of arteriovenous fistulas in patients with renal failure. Radiology 2012;265:584–590.

43. Cohen AT, Agnelli G, Anderson FA, et al. Venous thromboembolism (VTE) in Europe. The number of VTE events and associated morbidity and mortality. Thromb Haemost 2007;98:756–764.

44. Enden T, Storas TH, Negard A, et al. Visualization of deep veins and detection of deep vein thrombosis (DVT) with balanced turbo field echo (b-TFE) and contrast-enhanced T1 fast field echo (CE-FFE) using a blood pool agent (BPA). J Magn Reson Imaging 2010;31:416–424.

45. Hansch A, Betge S, Poehlmann G, et al. Combined magnetic resonance imaging of deep venous thrombosis and pulmonary arteries after a single injection of a blood pool contrast agent. Eur Radiol 2011;21:318–325.

46. Li W, Salanitri J, Tutton S, et al. Lower extremity deep venous thrombosis: evaluation with ferumoxytol-enhanced MR imaging and dual-contrast mechanism—preliminary experience. Radiology 2007;242:873–881.

47. Lim ST, Sohn MH, Kwak JY, Yim CY. Multiple hepatic adenomas: Tc-99m RBC liver SPECT findings with pathologic correlation. Clin Nucl Med 2002;27:270–274.

48. Schillaci O, Danieli R, Manni C, Capoccetti F, Simonetti G. Technetium-99m-labelled red blood cell imaging in the diagnosis of hepatic haemangiomas: the role of SPECT/CT with a hybrid camera. Eur J Nucl Med Mol Imaging 2004;31:1011–1015.

49. Martinez-Lazaro R, Dominguez P, Pascau J, Bittini A, Lafuente J, Desco M. Usefulness of Tc-99m RBC SPECT/MRI fusion imaging in small suspected hepatic hemangiomas. Clin Nucl Med 2004;29:844–845.

50. Milot L, Haider M, Foster L, McGregor C, Law C. Gadofosveset trisodium in the investigation of focal liver lesions in noncir-

rhotic liver: Early experience. J Magn Reson Imaging 2012;36: 738–742.

51. Hanna RF, Kased N, Kwan SW, et al. Double-contrast MRI for accurate staging of hepatocellular carcinoma in patients with cirrhosis. AJR Am J Roentgenol 2008;190:47–57.

52. Muhi A, Ichikawa T, Motosugi U, et al. Diagnosis of colorectal hepatic metastases: Contrast-enhanced ultrasonography versus contrast-enhanced computed tomography versus superparamagnetic iron oxide-enhanced magnetic resonance imaging with diffusion-weighted imaging. J Magn Reson Imaging 2010;32: 1132–1140.

53. Okada T, Sasaki F, Kamiyama T, et al. Focal nodular hyperplasia of the liver: usefulness of superparamagnetic iron oxide-enhanced magnetic resonance imaging. J Pediatr Surg 2005;40: E21–25.

54. Gunn AJ, Seethamraju RT, Hedgire S, Elmi A, Daniels GH, Harisinghani MG. Imaging behavior of the normal adrenal on ferumoxytol-enhanced MRI: preliminary findings. AJR Am J Roentgenol 2013;201:117–121.

55. Sielska M, Przanowski P, Wylot B, et al. Distinct roles of CSF family cytokines in macrophage infiltration and activation in glioma progression and injury response. J Pathol 2013;230:310–321.

56. Hamilton BE, Nesbit GM, Dosa E, et al. Comparative analysis of ferumoxytol and gadoteridol enhancement using T1- and T2-weighted MRI in neuroimaging. AJR Am J Roentgenol 2011;197: 981–988.

57. Farrell BT, Hamilton BE, Dosa E, et al. Using iron oxide nanoparticles to diagnose CNS inflammatory diseases and PCNSL. Neurology 2013;81:256–263.

58. Chalouhi N, Dumont AS, Randazzo C, et al. Management of incidentally discovered intracranial vascular abnormalities. Neurosurg Focus 2011;31:E1.

59. Jayaraman T, Berenstein V, Li X, et al. Tumor necrosis factor alpha is a key modulator of inflammation in cerebral aneurysms. Neurosurgery 2005;57:558–564; discussion 64.

60. Jayaraman T, Paget A, Shin YS, et al. TNF-alpha-mediated inflammation in cerebral aneurysms: a potential link to growth and rupture. Vasc Health Risk Manag 2008;4:805–817.

61. Chalouhi N, Ali MS, Jabbour PM, et al. Biology of intracranial aneurysms: role of inflammation. J Cereb Blood Flow Metab 2012;32:1659–1676.

62. Hasan D, Chalouhi N, Jabbour P, et al. Early change in ferumoxytol-enhanced magnetic resonance imaging signal suggests unstable human cerebral aneurysm: a pilot study. Stroke 2012;43:3258–3265.

63. Hasan DM, Chalouhi N, Jabbour P, Magnotta VA, Kung DK, Young WL. Imaging aspirin effect on macrophages in the wall of human cerebral aneurysms using ferumoxytol-enhanced MRI: preliminary results. J Neuroradiol 2013;40:187–191.

64. Hasan DM, Chalouhi N, Jabbour P, et al. Evidence that acetylsalicylic acid attenuates inflammation in the walls of human cerebral aneurysms: preliminary results. J Am Heart Assoc 2013;2:e000019.

65. Chen Y, Zhu W, Bollen AW, et al. Evidence of inflammatory cell involvement in brain arteriovenous malformations. Neurosurgery 2008;62:1340–1349; discussion 1349–1350.

66. Chen Y, Pawlikowska L, Yao JS, et al. Interleukin-6 involvement in brain arteriovenous malformations. Ann Neurol 2006;59:72–80.

67. Gaigalaite V, Ozheraitene V, Kalibatene D, Laurikenas K, Sabaliauskene Z. [Association between structure of atherosclerotic plaques in carotid arteries and myocardial infarction.] Kardiologiia 2013;53:21–25.

68. Pinelli A, Trivulzio S, Rossoni G, Redaelli R, Brenna S. Factors involved in sudden coagulation observed in patients with acute myocardial infarction. In Vivo 2012;26:1021–1025.

69. Marnane M, Prendeville S, McDonnell C, et al. Plaque inflammation and unstable morphology are associated with early stroke recurrence in symptomatic carotid stenosis. Stroke 2014;45: 801–806.

70. Tahara N, Tahara A, Honda A, et al. Molecular imaging of vascular inflammation. Curr Pharm Des 2013;20:2439–2437.

71. Libby P, Aikawa M. Stabilization of atherosclerotic plaques: new mechanisms and clinical targets. Nat Med 2002;8:1257–1262.

72. Libby P. Current concepts of the pathogenesis of the acute coronary syndromes. Circulation 2001;104:365–372.

73. Naghavi M, Libby P, Falk E, et al. From vulnerable plaque to vulnerable patient: a call for new definitions and risk assessment strategies: Part I. Circulation 2003;108:1664–1672.

74. Stary HC, Chandler AB, Dinsmore RE, et al. A definition of advanced types of atherosclerotic lesions and a histological classification of atherosclerosis. A report from the Committee on Vascular Lesions of the Council on Arteriosclerosis, American Heart Association. Circulation 1995;92:1355–1374.

75. Schmitz SA, Coupland SE, Gust R, et al. Superparamagnetic iron oxide-enhanced MRI of atherosclerotic plaques in Watanabe hereditable hyperlipidemic rabbits. Invest Radiol 2000;35:460–471.

76. Schmitz SA, Taupitz M, Wagner S, Wolf KJ, Beyersdorff D, Hamm B. Magnetic resonance imaging of atherosclerotic plaques using superparamagnetic iron oxide particles. J Magn Reson Imaging 2001;14:355–361.

77. Schmitz SA, Taupitz M, Wagner S, et al. Iron-oxide-enhanced magnetic resonance imaging of atherosclerotic plaques: postmortem analysis of accuracy, inter-observer agreement, and pitfalls. Invest Radiol 2002;37:405–411.

78. Kooi ME, Cappendijk VC, Cleutjens KB, et al. Accumulation of ultrasmall superparamagnetic particles of iron oxide in human atherosclerotic plaques can be detected by in vivo magnetic resonance imaging. Circulation 2003;107:2453–2458.

79. Herborn CU, Vogt FM, Lauenstein TC, et al. Magnetic resonance imaging of experimental atherosclerotic plaque: comparison of two ultrasmall superparamagnetic particles of iron oxide. J Magn Reson Imaging 2006;24:388–393.

80. Li X, Kramer MC, van der Loos CM, et al. A pattern of disperse plaque microcalcifications identifies a subset of plaques with high inflammatory burden in patients with acute myocardial infarction. Atherosclerosis 2011;218:83–89.

81. Bobryshev YV, Killingsworth MC, Lord RS, Grabs AJ. Matrix vesicles in the fibrous cap of atherosclerotic plaque: possible contribution to plaque rupture. J Cell Mol Med 2008;12:2073–2082.

82. Li W, Ostblom M, Xu LH, et al. Cytocidal effects of atheromatous plaque components: the death zone revisited. FASEB J 2006;20:2281–2290.

83. Wagner S, Schnorr J, Ludwig A, et al. Contrast-enhanced MR imaging of atherosclerosis using citrate-coated superparamagnetic iron oxide nanoparticles: calcifying microvesicles as imaging target for plaque characterization. Int J Nanomed 2013;8:767–779.

84. Mumprecht V, Detmar M. Lymphangiogenesis and cancer metastasis. J Cell Mol Med 2009;13:1405–1416.

85. Foster PJ, Dunn EA, Karl KE, et al. Cellular magnetic resonance imaging: in vivo imaging of melanoma cells in lymph nodes of mice. Neoplasia 2008;10:207–216.

86. Cserni G. Metastases in axillary sentinel lymph nodes in breast cancer as detected by intensive histopathological work up. J Clin Pathol 1999;52:922–924.

87. Anzai Y, Piccoli CW, Outwater EK, et al. Evaluation of neck and body metastases to nodes with ferumoxtran 10-enhanced MR imaging: phase III safety and efficacy study. Radiology 2003;228:777–788.

88. Koh DM, Brown G, Temple L, et al. Rectal cancer: mesorectal lymph nodes at MR imaging with USPIO versus histopathologic findings—initial observations. Radiology 2004;231:91–99.

89. Harisinghani MG, Saini S, Weissleder R, et al. MR lymphangiography using ultrasmall superparamagnetic iron oxide in patients with primary abdominal and pelvic malignancies: radiographic-pathologic correlation. AJR Am J Roentgenol 1999;172:1347–1351.

90. Heesakkers RA, Jager GJ, Hovels AM, et al. Prostate cancer: detection of lymph node metastases outside the routine surgical area with ferumoxtran-10-enhanced MR imaging. Radiology 2009;251:408–414.

91. Guimaraes R, Clement O, Bittoun J, Carnot F, Frija G. MR lymphography with superparamagnetic iron nanoparticles in rats: pathologic basis for contrast enhancement. AJR Am J Roentgenol 1994;162:201–207.

92. Tatsumi Y, Tanigawa N, Nishimura H, et al. Preoperative diagnosis of lymph node metastases in gastric cancer by magnetic resonance imaging with ferumoxtran-10. Gastric Cancer 2006;9:120–128.

93. Rockall AG, Sohaib SA, Harisinghani MG, et al. Diagnostic performance of nanoparticle-enhanced magnetic resonance imaging in the diagnosis of lymph node metastases in patients with endometrial and cervical cancer. J Clin Oncol 2005;23:2813–2821.

94. Motomura K, Izumi T, Tateishi S, et al. Correlation between the area of high-signal intensity on SPIO-enhanced MR imaging and the pathologic size of sentinel node metastases in breast cancer patients with positive sentinel nodes. BMC Med Imaging 2013;13:32.

95. McDermott S, Thayer SP, Fernandez-Del Castillo C, Mino-Kenudson M, Weissleder R, Harisinghani MG. Accurate prediction of nodal status in preoperative patients with pancreatic ductal adenocarcinoma using next-gen nanoparticle. Transl Oncol 2013;6:670–675.

96. Neuwelt EA, Varallyay CG, Manninger S, et al. The potential of ferumoxytol nanoparticle magnetic resonance imaging, perfusion, and angiography in central nervous system malignancy: a pilot study. Neurosurgery 2007;60:601–611; discussion 611–612.

97. Varallyay CG, Muldoon LL, Gahramanov S, et al. Dynamic MRI using iron oxide nanoparticles to assess early vascular effects of antiangiogenic versus corticosteroid treatment in a glioma model. J Cereb Blood Flow Metab 2009;29:853–860.

98. Thompson EM, Guillaume DJ, Dosa E, et al. Dual contrast perfusion MRI in a single imaging session for assessment of pediatric brain tumors. J Neurooncol 2012;109:105–114.

99. Gruessner AC, Sutherland DE, Gruessner RW. Long-term outcome after pancreas transplantation. Curr Opin Organ Transplant 2012;17:100–105.

100. Toso C, Isse K, Demetris AJ, et al. Histologic graft assessment after clinical islet transplantation. Transplantation 2009;88:1286–1293.

101. Jirak D, Kriz J, Herynek V, et al. MRI of transplanted pancreatic islets. Magn Reson Med 2004;52:1228–1233.

102. Borot S, Crowe LA, Parnaud G, et al. Quantification of islet loss and graft functionality during immune rejection by 3-Tesla MRI in a rat model. Transplantation 2013;96:438–444.

103. Khurana A, Nejadnik H, Chapelin F, et al. Ferumoxytol: a new, clinically applicable label for stem-cell tracking in arthritic joints with MRI. Nanomedicine (Lond) 2013;8:1969–1983.

104. Khurana A, Chapelin F, Beck G, et al. Iron administration before stem cell harvest enables MR imaging tracking after transplantation. Radiology 2013;269:186–197.